A Probabilistic Distance-Based Modeling and Analysis for Cellular Networks With Underlaying Device-to-Device Communications

Fei Tong, *Student Member, IEEE*, Ying Wan, Lei Zheng, Jianping Pan, *Senior Member, IEEE*, and Lin Cai, *Senior Member, IEEE*

***Abstract*— Device-to-device (D2D) communications in cellular networks are promising technologies for improving network performance. However, they may cause severe intra/inter-cell interference that can considerably degrade the performance of cellular users, and vice versa. Therefore, interference analysis has been one of the most important research topics in such a system. Focusing on an uplink resource reusing scenario, this paper presents a framework based on a probabilistic distance and path-loss model to obtain the distributions of signal, interference, and further Signal-to-Interference-plus-Noise Ratio (SINR), based on which, the performance metrics that are functions of SINR can be analyzed, such as outage probability and capacity. Different from the previous work, this proposed framework: 1) obtains interference and SINR distributions for both cellular and D2D communications, through which insights into their performance metrics and mutual influence are provided and 2) has no limitations on cell shapes, except that they are approximated by polygons or circles. The framework can also be applied to a downlink reusing scenario. Our results indicate that the developed framework is helpful for network planners to effectively tune the network parameters, and thus to achieve the optimum system performance for both cellular and D2D communications.**

***Index Terms*— Cellular networks, D2D communications, interference, signal-to-interference ratio, probabilistic distance model.**

I. Introduction

To address the big challenges raised by the tremendous increase of mobile devices and explosive growth of data traffic demands in cellular networks [1], a lot of technologies have been studied and developed in the last decade, such as white space [2], cognitive radio [3], femtocells [4], Device-to-Device (D2D) communications [5], etc. Recently, great efforts have been devoted from both academia and industry to the research and development of D2D communications, as believed to be one of the promising technologies to improve network performance in several aspects. Specifically, by allowing the direct communications between nearby User Equipments (UEs) without traversing the Base Station (BS) or core network, not only are the transmission delay and power reduced, but also the network coverage can be extended. More importantly, D2D communications in cellular networks occurring on either the cellular or unlicensed/unused spectrum bring a great chance to improve network capacity and spectrum efficiency.

One of the serious challenges facing the implementation of D2D communications in cellular networks is the possible interference between D2D and cellular links and that between D2D links due to spectrum sharing. For example, in a scenario where the D2D UEs (DUEs) reuse the uplink cellular resources, a D2D communication might be affected by a simultaneous transmission from a Cellular UE (CUE) to the BS. In particular, as the number of concurrent D2D pairs increases, not only will the quality of the received signal at the BS be highly affected by the accumulated interference from the transmitting DUEs, but also the performance of each D2D pair itself will be degraded due to the inter-D2D interference. Likewise, in a downlink reusing scenario, the transmitting DUEs may make nearby CUEs fail to receive any signal. Therefore, the interference analysis in such a system is of great importance. An accurate analysis of interference can provide us with deep insights into system performance in terms of several important performance metrics, such as Signal-to-Interference-plus-Noise Ratio (SINR) and those which are functions of SINR, including outage probability, capacity, etc.

In light of the significance of the interference analysis in cellular networks with D2D communications, extensive research has been conducted. Existing work mainly focused on either a simple scenario with single D2D pair [6]–[8] or throughput bound analysis [9], [10]. Recently, the tools from stochastic geometry have been adopted for the interference analysis of D2D communications in a large-scale cellular system with multiple cells working on the same frequency band [11], [12]. As detailed in the next section, however, these results cannot apply directly to a system with pre-deployed BSs according to cell planning, higher frequency

Manuscript received February 4, 2016; revised June 9, 2016, August 18, 2016, and October 24, 2016; accepted October 30, 2016. Date of publication November 4, 2016; date of current version January 6, 2017. This work was supported in part by the Natural Sciences and Engineering Research Council of Canada, in part by the Canada Foundation for Innovation, in part by the British Columbia Knowledge Development Fund, and in part by the Ministry of Educations Key Lab for Computer Network and Information Integration, Southeast University, China. The associate editor coordinating the review of this paper and approving it for publication was R. Zheng.

F. Tong and J. Pan are with the Department of Computer Science, University of Victoria, Victoria, BC V8P 5C2, Canada (e-mail: tongfei@uvic.ca; pan@uvic.ca).

Y. Wan is with the Department of Computer Science, Tsinghua University, Beijing, China (e-mail: wany16@mails.tsinghua.edu.cn).

L. Zheng and L. Cai are with the Department of Electrical and Computer Engineering, University of Victoria, Victoria, BC V8P 5C2, Canada (e-mail: zhengl@uvic.ca; cai@uvic.ca).

Color versions of one or more of the figures in this paper are available online at http://ieeexplore.ieee.org.

Digital Object Identifier 10.1109/TWC.2016.2625301

reuse factors, or sector-partitioned cells. How to quantify the interference and system performance in more general scenarios is still an open issue, inspiring the work in this paper as a significant complementary one to the existing approaches and results.

Different from the existing work, this paper proposes a new analytical framework based on a probabilistic distance and path-loss model to obtain the distributions of signal, interference, and SINR in a cellular network with underlaying D2D communications. Since uplink resources are more likely to be shared than downlink resources as a result of the asymmetric uplink and downlink service loads [13], [14], under-utilization of uplink spectrum [15], and stronger abilities at BSs to process interference than at CUEs [14], the framework focuses on an uplink reusing scenario, where multiple DUEs reuse the uplink resource of a CUE. Specifically, according to a general path-loss model commonly adopted for analyzing wireless networks, the signal/interference received at a node depends heavily on the distances to its transmitting/interfering nodes. Considering that the UEs are independently and uniformly distributed in a cell, we first obtain the distributions of the distance from the BS to a random UE and that between two random UEs, associated with arbitrarily-shaped service areas. The technique can be extended to non-uniformly distributed UEs. The case that a guard region (GR) is set for the BS to mitigate the interference from DUEs is also considered, where DUEs are randomly deployed beyond the GR. Meanwhile, the shadowing and fading effects can also be easily included, as shown in Section VI, and the proposed framework can also be applied to a downlink reusing scenario, as detailed in Section V.

The main contributions of this paper are as follows. First, the proposed framework has no limitations on the shapes of both the cells and GRs, and a cellular system with multiple cells can also be analyzed. For the distribution of the distance from a reference point to a random one, we adopt the approach proposed in our technical report in [16], which can handle arbitrarily-shaped polygons and has no limitations on the location of the reference point (i.e., the BS, thus, in an uplink reusing scenario with multiple cells, the interference to the BS from the DUEs in its neighbor cells can also be analyzed). Meanwhile, for the distribution of the distance between two random points, we adopt the systematic approach proposed by us in [17] that can handle arbitrary convex, concave, and ring geometries, as well as disjoint geometries (thus the inter-cell/sector interference can also be analyzed in a multi-cell network or sector-partitioned cell). Second, with the obtained distance distributions, we accurately model and analyze a cellular network with multiple concurrent D2D pairs in an uplink reusing scenario. The distributions of the received signal, interference, and SINR are then derived, and further the interference and outage probabilities for both cellular and D2D communications are thoroughly investigated. The results presented can provide important insights and guidelines for network planning and dimensioning at the system level, e.g., on average, how many concurrent D2D pairs can be allowed and how large a GR can be set, by considering the bounded outage probabilities for both cellular and D2D communications systematically and comprehensively.

The rest of the paper is organized as follows. Section II summarizes the related work on the interference analysis for D2D communications. Section III presents the system model. The approaches to obtaining the distance and SINR distributions are detailed in Section IV. Section V shows the applicability of the framework to downlink resource reusing, inter-cell interference, sector-partitioned cells, irregular cells/GRs, and non-uniform UE distribution. Performance evaluation is conducted in Section VI. Finally, Section VII concludes the paper.

II. Related Work

There have been great research efforts in obtaining the performance metrics for D2D communications in cellular networks based on interference analysis. For example, [6] studied the uplink capacity gain when a D2D link is enabled in an FDD CDMA-based cellular network. In [7], an Interference-Limited Area (ILA) control scheme for an uplink reusing scenario was proposed to manage the interference from the CUE to a D2D transmission when multiple antennas are used by the BS. By analyzing the coverage of the ILA for one D2D pair, a lower bound of the ergodic capacity was derived. After that, an extended approach was proposed in [8] to take into consideration a downlink reusing scenario. Reference [18] presented a distance-based study on the evaluation of D2D communication. Overall, these works assumed that there is only one D2D pair in a cell either to avoid harmful interference to the cellular transmissions in the cell or due to the intrinsic limitation of the proposed model, and thus their results cannot be directly applied to the scenario with multiple concurrent D2D pairs.

Recent works begin to consider the interference from multiple D2D pairs accumulated at the BS in a cell. For example, [11] studied the effect of the Successive Interference Cancellation (SIC) technique, aiming to reduce/control interference and improve network capacity, in a D2D-enabled, multi-cell cellular network. By using the tools from stochastic geometry, the successful transmission probabilities for both the cellular uplinks and D2D links with SIC were derived. In [12], an uplink reusing scenario in a multi-cell, OFDMA-based cellular network was considered. Both the GRs approximated as circles centered at each BS and an open-loop fraction power control scheme were adopted to mitigate the D2D-to-cellular interference. Also with stochastic geometry, the outage probabilities of both CUEs and DUEs and the area spectral efficiency of the whole hybrid network were explored. To simplify the analysis, the model assumed that the D2D transmitter and its intended receiver in a pair have a constant distance, which might be impractical due to the randomness of DUE locations. In summary, these works considered a large-scale cellular system with multiple cells working on the same frequency band (i.e., the frequency reuse factor is 1). With the tools from stochastic geometry, BSs were assumed to be deployed randomly following a Poisson Point Process (PPP), whereas in reality BSs are deployed according to cell planning and their locations are not totally random. Especially, in a scenario with a higher frequency reuse factor, e.g., 7, where it needs to investigate the performance metrics of a single

cell, or for a sector-partitioned cell where the BS is equipped with multiple directional antennas [10], their results are not applicable directly.

As an another example with stochastic geometry, [19] analyzed the spatial constraints of DUEs in a single-cell, uplink reusing scenario. Depending on whether there is a GR for the BS and the BS serving zone is infinite or not, four kinds of network models were discussed. Both the cell and GR were modeled as circles. For the cumulative interference to the BS, only the D2D transmitters located at a fixed distance from the BS were considered. To analyze the success probability of D2D transmissions, the model assumed that the transmission power of the CUE is no larger than that of DUE, which might be impractical since the DUE transmission power is usually much smaller than the CUE's. In addition, for the finite coverage case, the model only worked out the success probability of the CUE transmission.

For the D2D throughput bound analysis, a geometrical-based method was proposed in [9] considering an uplink reusing scenario. Three guard distances from a DUE, respectively to the BS, to the CUE, and to the other communicating DUEs were obtained by considering the SINR requirements for both cellular and D2D transmissions. Then the maximum number of concurrent D2D pairs was approximated, and further the D2D throughput bound was derived. The bound analysis was then extended in [10] to analyze the interference accumulated at the BS and receiving DUEs.

Recently, there are increasing studies on the utilization of distance distributions for performance analysis in wireless networks. In [20], the total interference received at a BS in a cell from the transmissions in its neighbor cells was obtained based on the distance distributions associated with regular hexagons. A general framework based on the distance distributions associated with arbitrary shapes was proposed in [21] to analyze the outage probability in finite wireless networks. For tiered cellular networks, our recent work [22] utilized distance distributions to analyze the outage probability for the macro and femto BSs in arbitrarily-shaped cells. Overall, they are all based on the distribution of the distance between a given reference point (e.g., the BS or a given reference receiver) and a random point. For analyzing the underlaying D2D communications in cellular networks in this paper, however, the above approaches/results are not applicable, since all DUEs are randomly distributed and thus the distribution of the distance between two random points has to be involved.

III. System Model

The system model considered in this paper is shown in Fig. 1, where the UEs are independently and uniformly distributed within a polygonal cell (the non-uniform UE distribution can also be considered as discussed in Section V). A higher frequency reuse factor is considered, so that the neighbour cells are in orthogonal channels. To ensure the generality and applicability of our approach, the cell is shown with an arbitrary polygonal shape. CUEs communicate with the BS in either uplink or downlink mode with a transmission power of P_C. In the uplink mode, CUEs transmit to the BS, while the direction is reversed in the downlink mode. On the other hand, DUEs exchange data directly by utilizing either the uplink or downlink cellular resources with a transmission power of P_D. Since uplink resources are more likely to be shared than downlink resources due to the asymmetric uplink and downlink service loads, under-utilization of uplink spectrum, and stronger abilities at BSs to process interference than at CUEs [13]–[15], this paper focuses on an uplink reusing scenario, in which one CUE and N concurrent D2D pairs are transmitting simultaneously reusing the uplink resource of the CUE. Note that the active CUE location is random at a given time. For multiple CUEs in orthogonal channels, the proposed framework applies to each of them. For a downlink reusing scenario, our approach still applies, as explained in Section V. A D2D connection will be established only when the distance between two DUEs is within a predefined range $[d_{\min}^{D2D}, d_{\max}^{D2D}]$. Depending on whether or not there is a GR set for the BS to guarantee the successful transmission from the CUE to the BS, two scenarios are considered: 1) no GR set for the BS, as shown in Figure 1(a); 2) a GR set for the BS, as shown in Figure 1(b). For the latter case, the D2D communications only happen outside the GR, whereas the active CUE can be anywhere within the cell. In this paper, we will conduct a physical interference model-based performance analysis, which focuses on the cumulative interference at a specific receiver.

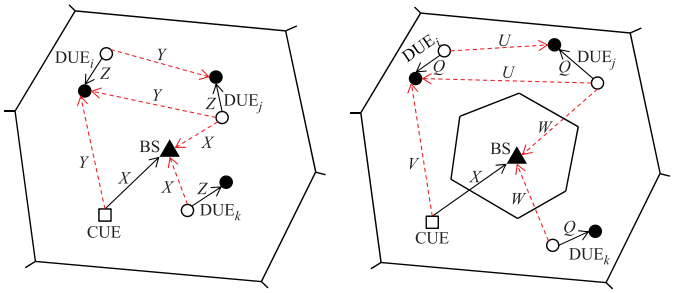

(a) No GR for the BS (b) A GR for the BS

Fig. 1. System model consisting of several D2D pairs (shown as circles) underlaying a cell (shown as an irregular polygon) with one CUE (shown as a square, which can be anywhere in the cell region) in an uplink reusing scenario, where the solid black arrow lines show the transmission between two DUEs or between the CUE and BS, and the dashed red arrow lines show the interference at a receiver from an unintended transmitter. Note that not all of the unintended transmitters' interference is shown for a receiver. The random variables beside each arrow line are introduced in Section IV and listed in Table I.

Considering that the signal power is attenuated with distance [23], a general path-loss model is applied to characterize the received SINR at either the BS or a DUE receiver and link capacity (the model can be easily extended to consider shadowing and fading as shown below). Specifically, the received SINR at the BS from the CUE is

$$SINR_B = \frac{K P_C d_0^{\alpha} d_{CUE,BS}^{-\alpha}}{N_0 W + I_B}, \tag{1}$$

and the corresponding link capacity is

$$C_B = W \log_2(1 + SINR_B), \tag{2}$$

where K is the antenna- and processing gain-related parameter, d_0 is the reference distance, α is the path-loss exponent, $d_{CUE,BS}$ is the distance between the CUE and the BS, W is the communication bandwidth, N_0 is the one-sided spectral density of additive white Gaussian noise, and I_B is the cumulative interference at the BS from all DUE transmitters and we have

$$I_B = K P_D {d_0}^{\alpha} \sum_i {d_{DUE_{i\_TX},BS}}^{-\alpha}, \tag{3}$$

where $d_{DUE_{i\_TX},BS}$ is the distance between the DUE transmitter in the ith D2D pair and the BS.

Likewise, the received SINR at the DUE receiver of the ith D2D pair from the DUE transmitter in the same pair is

$$SINR_{Di} = \frac{K P_D {d_0}^{\alpha} {d_{DUE_{i\_TX},DUE_{i\_RX}}}^{-\alpha}}{N_0 W + I_{Di}}, \tag{4}$$

and the corresponding link capacity is

$$C_{Di} = W \log_2(1 + SINR_{Di}), \tag{5}$$

where $d_{DUE_{i\_TX},DUE_{i\_RX}}$ is the distance between the DUE transmitter and receiver of the ith D2D pair, and I_{Di} is the cumulative interference received at the DUE receiver of the ith D2D pair, which consists of two parts, namely, the interference from the CUE, I'_{Di}, and the cumulative interference from all other D2D pairs except pair i, I''_{Di}, and we have

$$I_{Di} = I'_{Di} + I''_{Di}, \tag{6}$$

$$I'_{Di} = K P_C {d_0}^{\alpha} {d_{CUE,DUE_{i\_RX}}}^{-\alpha}, \tag{7}$$

$$I''_{Di} = K P_D {d_0}^{\alpha} \sum_{j \neq i} {d_{DUE_{j\_TX},DUE_{i\_RX}}}^{-\alpha}, \tag{8}$$

where $d_{CUE,DUE_{i\_RX}}$ is the distance between the CUE and the DUE receiver of the ith D2D pair, and $d_{DUE_{j\_TX},DUE_{i\_RX}}$ is the distance between the DUE receiver of the ith D2D pair and the DUE transmitter of a D2D pair other than i.

From (1)–(8), it is obvious that the distance between a UE (DUE/CUE) and the BS and that between two UEs play significant roles. Since signal and interference are non-linear functions of inter-node distances, not only their mean values but also their distributions are needed to obtain the statistics of SINRs using (1) and (4), all based on the distributions of the distances mentioned above. With the obtained SINR statistics, the performance metrics of the system, such as outage probability and link capacity, can be quantified effectively.

In the next section, we will show in detail how to obtain

- the distribution of the distance from a reference point (e.g., the BS) to a random point (e.g., a CUE/DUE), for obtaining the distribution of the SINR at the BS,
- the distribution of the distance between two random points (e.g., DUE–DUE or CUE–DUE), for obtaining the distribution of the SINR at a DUE receiver, and
- the distribution of the SINR at either the BS or a DUE receiver based on the obtained distance distributions.

IV. Approaches to Distance, Interference, SINR, and Link Capacity Distributions

According to our model, the Random Variables (RVs) shown in Fig. 1 for the distances in (1)–(8) are listed in Table I, along with their Cumulative Distribution Functions (CDFs). Depending on whether or not there is a GR set for the BS to guarantee its reception from the CUE, all the involved distances will have different distributions except $d_{CUE,BS}$, since the GR only affects the locations of DUEs. For the case without GR, considering the randomness of the locations of all the UEs in the cell, the distance between the CUE and BS and that between a DUE transmitter and the BS can be viewed as i.i.d. RVs (both denoted as X), and the same for the distance between the CUE and a DUE receiver and that between a DUE transmitter and a DUE receiver which are in different D2D pairs (both denoted as Y). For the two DUEs that can communicate with each other and form a D2D pair, the distance between them (RVs Z or Q) has a different distribution from that of Y or U, due to the D2D communication range limit, i.e., $[d_{\min}^{D2D}, d_{\max}^{D2D}]$. As mentioned in the last section, the SINR at the BS involves the distance from a reference point to a random point, and that at a DUE receiver involves the distance between two random points. With such a classification, we next detail how to obtain the CDFs of the above RVs.

TABLE I
Random Variables and Their CDFs for the Distances in (1)–(8)

	Distance	RV (CDF)	
		No GR	With GR
SINR at the BS	$d_{CUE,BS}$ in (1)	$X\ (F_X(d))$	$X\ (F_X(d))$
	$d_{DUE_{i\_TX},BS}$ in (3)	$X\ (F_X(d))$	$W\ (F_W(d))$
SINR at a DUE receiver	$d_{DUE_{i\_TX},DUE_{i\_RX}}$ in (4)	$Z\ (F_Z(d))$	$Q\ (F_Q(d))$
	$d_{CUE,DUE_{i\_RX}}$ in (7)	$Y\ (F_Y(d))$	$V\ (F_V(d))$
	$d_{DUE_{j\_TX},DUE_{i\_RX}}$ in (8)	$Y\ (F_Y(d))$	$U\ (F_U(d))$

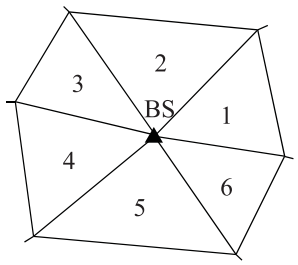

Fig. 2. Triangulation from the BS.

A. Distance From a Reference Point to a Random Point

1) $F_X(d)$: To obtain $F_X(d)$, the approach proposed in our technical report in [16] is adopted. According to [16], the distribution of the distance from a vertex of an arbitrarily-shaped triangle to a random point inside that triangle is first obtained. Then the arbitrary polygonal cell can be triangulated with respect to the BS (i.e., the reference point). For example, in Fig. 2, there are 6 triangles generated after triangulation. Let $F_{\triangle i}(d)$ denote the CDF of the distribution of the distance from the BS to a random point inside the ith triangle. $F_X(d)$ can be obtained by a weighted probabilistic sum of the distributions of

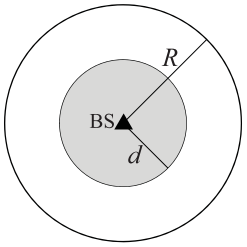

Fig. 3. $F_{X'}(d)$.

the distance from the BS to each of the triangles that constitute the cell,

$$F_X(d) = \sum_{i}^{K} \frac{S_i}{S} F_{\triangle i}(d), \tag{9}$$

where K is the number of triangles generated after the triangulation with respect to the BS, S_i is the area of the ith triangle, and S is the area of the cell.

2) $F_W(d)$: Due to the effect of the GR, $F_W(d)$ is different from $F_X(d)$. Given that the GR has also a polygonal shape as shown in Fig. 1(b), we can first obtain the CDF of the distribution of the distance from the BS to a random point inside the GR, denoted as $F_G(d)$, by also using (9). In a simple assumption where the GR is approximated by a circle with radius of R and centered at the BS, as shown in Fig. 3, $F_G(d)$ can be obtained by using the area-ratio approach,

$$F_G(d) = \begin{cases} \dfrac{d^2}{R^2}, & 0 \le d \le R \\ 1, & d \ge R. \end{cases} \tag{10}$$

Let S_{GR} denote the area of the GR and $S_{\widetilde{GR}}$ the area of the region (or ring, denoted as $\widetilde{\text{GR}}$) which is beyond the GR but within the cell. The area of the cell is S. The possibility that the random point appears in the GR is $\frac{S_{GR}}{S}$, while $\frac{S_{\widetilde{GR}}}{S}$ in the $\widetilde{\text{GR}}$. Therefore, with a weighted probabilistic sum, we have

$$F_X(d) = \frac{S_{GR}}{S} F_G(d) + \frac{S_{\widetilde{GR}}}{S} F_W(d). \tag{11}$$

Thus, $F_W(d)$ can be obtained.

Note that if there are nodes deployed uniformly at random in the GR and $\widetilde{\text{GR}}$ but with different node densities, the above weighted probabilistic sum is still applicable, but with the weights modified correspondingly due to the node density differences. Specifically, assuming the node density ratio between the GR and $\widetilde{\text{GR}}$ is $\lambda_1 : \lambda_2$ (λ_1 and λ_2 are not zero at the same time),

$$F_X(d) = \frac{S_{GR}\lambda_1}{S_{GR}\lambda_1 + S_{\widetilde{GR}}\lambda_2} F_G(d) + \frac{S_{\widetilde{GR}}\lambda_2}{S_{GR}\lambda_1 + S_{\widetilde{GR}}\lambda_2} F_W(d), \tag{12}$$

Especially, if $\lambda_1 : \lambda_2 = 1 : 1$, i.e., both areas have the same node density, then $F_X(d)$ is just what shown in (11). Therefore, the proposed approach in [16] has a potential of handling the networks with non-uniform nodal distributions.

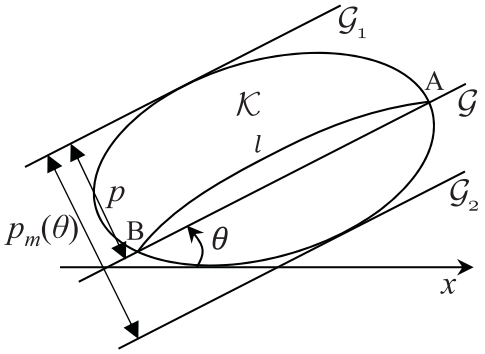

Fig. 4. Convex geometry.

B. Distance Between Two Random Points

It becomes much more challenging to obtain the corresponding distance distribution due to the randomness of both points, especially for the case where the cell has an arbitrary irregular shape in our model, and a GR may be set for the BS, i.e., another arbitrarily-shaped void area inside (hereafter, we call a geometry containing a void area a "ring"). In this subsection, we first adopt the kinematic measure concept from integral geometry [24]–[26] to obtain the distribution of the distance between two random points within an arbitrary convex geometry. Then we extend the approach to disjoint, concave and ring geometries. Thus all the distance distributions required in our model can be obtained. Using the approach, we have obtained several distance distributions regarding arbitrary polygons (including triangles, pentagons, hexagons, etc.) and ring geometries. To save space, they are not shown here in this paper. We refer interested readers to our recent technical report in [17] for full details.

1) $F_Y(d)$ and $F_Z(d)$:

Definition 1 (Orientation of a Line): Without Loss Of Generality (WLOG), the orientation of a line is defined as θ ($0 \le \theta \le \pi$) which is the angle made by the part of the line above x-axis with the positive direction of the x-axis.

Definition 2 (Support Lines of a Convex Geometry in Orientation θ): Given a convex geometry, the support lines of the geometry in orientation θ are defined as the two tangents in orientation θ which completely encompass the whole geometry. An example for illustration is shown in Fig. 4, where $\mathcal{G}_1$ and $\mathcal{G}_2$ are two support lines of $\mathcal{K}$ in orientation θ.

Therefore, a line $\mathcal{G}$ intersecting with a convex geometry can be determined by its orientation θ and its distance p to one of the support lines in orientation θ, as shown in Fig. 4. The length of the chord of the geometry produced by $\mathcal{G}$ is denoted as $l(\theta, p)$ (we use l for the ease of presentation),[1] and the distance between the two support lines with the same orientation θ is denoted as $p_m(\theta)$. Then we have the following theorem,

Theorem 1: Denote $\mathcal{K}$ as an arbitrary convex geometry with area of S. The CDF of the distribution of the distance (denoted as an RV D) between any two points which are uniformly

[1]In the following, unless explicitly stated otherwise, l is equivalent to $l(\theta, p)$.

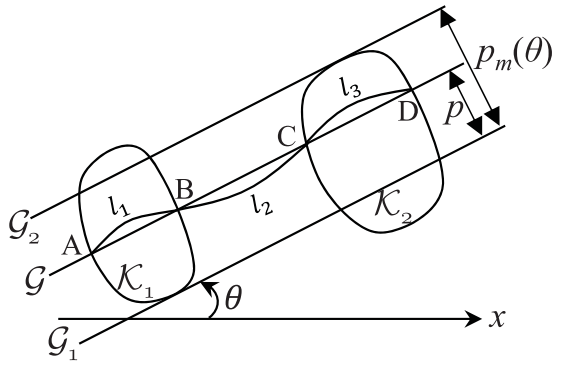

Fig. 5. Two random points, P_1 and P_2, respectively within two disjoint convex geometries, $\mathcal{K}_1$ and $\mathcal{K}_2$.

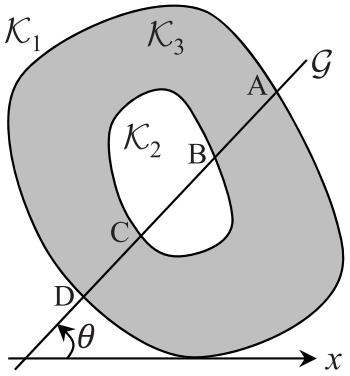

Fig. 6. Overlapped geometries.

distributed at random within $\mathcal{K}$ is

$$F_D(d) = \frac{1}{S^2}\int_0^{\pi}\int_0^{p_m(\theta)} F_{\mathcal{G}}(d)\ \mathrm{d}p\mathrm{d}\theta, \tag{13}$$

where

$$F_{\mathcal{G}}(d) = d^2 l - \frac{2}{3}d^3\ . \tag{14}$$

Proof: We refer interested readers to our technical report [17]. ∎

As a result, $F_Y(d)$ in our model can be obtained according to (13). Meanwhile, $F_Z(d)$ can be obtained based on $F_Y(d)$ by considering the D2D communication range,

$$F_Z(d) = \frac{F_Y(d) - F_Y(d_{\min}^{D2D})}{F_Y(d_{\max}^{D2D}) - F_Y(d_{\min}^{D2D})}\ . \tag{15}$$

2) $F_U(d)$, $F_V(d)$ and $F_Q(d)$:

Definition 3 (Support Lines of Two Disjoint Convex Geometries in Orientation θ): Suppose $\mathcal{K}_1$ and $\mathcal{K}_2$ are two disjoint convex geometries. The support lines of the two geometries in orientation θ are defined as the two parallel lines in orientation θ which intersect with the both geometries and are respectively tangent to $\mathcal{K}_1$ and $\mathcal{K}_2$, so that among all the lines in the same orientation θ, only those which are between the two support lines can intersect with the both geometries. An example for illustration is shown in Fig. 5, where $\mathcal{G}_1$ and $\mathcal{G}_2$ are two support lines of $\mathcal{K}_1$ and $\mathcal{K}_2$ in orientation θ.

Therefore, a line $\mathcal{G}$ intersecting with two disjoint convex geometries can still be determined by its orientation θ and its distance p to one of the support lines in the same orientation θ. As shown in Fig. 5, $\mathcal{G}$ intersecting with both $\mathcal{K}_1$ and $\mathcal{K}_2$ produces two chords with length of $|AB| = l_1$ and $|CD| = l_3$ inside $\mathcal{K}_1$ and $\mathcal{K}_2$, respectively, and a segment with length of $|BC| = l_2$ outside. Similarly,[2] l_1, l_2, and l_3 are also determined by (θ, p). $p_m(\theta)$ is the distance between the two support lines in orientation θ.

Theorem 2: The CDF of the distribution of the distance between two points which are uniformly distributed at random respectively within two disjoint convex geometries with areas of S_1 and S_2, respectively, is

$$F_D(d) = \frac{1}{S_1 S_2}\int_0^{\pi}\int_0^{p_m(\theta)} F_{\mathcal{G}}(d)\ \mathrm{d}p\mathrm{d}\theta, \tag{16}$$

where

$$F_{\mathcal{G}}(d) = \begin{cases} F_{\mathcal{G}}^{\mathrm{i}}(d), & l_2 \le d \le l_1 + l_2 \\ F_{\mathcal{G}}^{\mathrm{ii}}(d), & l_1 + l_2 \le d \le l_2 + l_3 \\ F_{\mathcal{G}}^{\mathrm{iii}}(d), & l_2 + l_3 \le d \le l_1 + l_2 + l_3, \end{cases} \tag{17}$$

where

$$F_{\mathcal{G}}^{\mathrm{i}}(d) = \frac{(l_2 - d)^2(l_2 + 2d)}{3}, \tag{18}$$

$$F_{\mathcal{G}}^{\mathrm{ii}}(d) = l_1(d + l_1 + l_2)(d - l_1 - l_2), \tag{19}$$

$$F_{\mathcal{G}}^{\mathrm{iii}}(d) = \frac{1}{6}(2l_2 + 2l_3 + d)(l_2 + l_3 - d)^2 - \frac{1}{2}\left((l_2 + l_3)^2 - d^2\right)(l_1 + l_2 + l_3 - d). \tag{20}$$

Proof: We refer interested readers to our technical report [17]. ∎

Based on the obtained results above, we can obtain the CDFs of the random distances associated with ring geometries, which are required to solve the case where a GR for the BS is involved in our model. Figure 6 shows a general case, where a geometry $\mathcal{K}_1$ has a small geometry $\mathcal{K}_2$ inside. Denote the grey region inside $\mathcal{K}_1$ but outside $\mathcal{K}_2$ as $\mathcal{K}_3$ (the ring). With the above approach, we can obtain the CDF of the random distances within $\mathcal{K}_1$ and that within $\mathcal{K}_2$, denoted as $F_{11}(d)$ and $F_{22}(d)$, respectively (hereafter, we use $F_{xx}(d)$ to denote the CDF of the random distances within $\mathcal{K}_x$, and $F_{xy}(d)$ or $F_{yx}(d)$ the CDF of the random distances between $\mathcal{K}_x$ and $\mathcal{K}_y$). To obtain the CDFs of RVs Q, U, and V in our model, we need to know $F_{33}(d)$ and $F_{13}(d)$. To this end, we first obtain $F_{23}(d)$, by using the approach to obtaining the CDF of the distance between two disjoint geometries as illustrated in Fig. 5 (a special case where l_2 is always zero).

As shown in Fig. 6, a line $\mathcal{G}$ with orientation θ and intersecting with $\mathcal{K}_2$ produces three segments, i.e., AB and CD inside $\mathcal{K}_3$, and BC inside $\mathcal{K}_2$. According to (17), we can find, say $F_{\mathcal{G}}^{a}(d)$, associated with the distance between AB and BC, and $F_{\mathcal{G}}^{b}(d)$ associated with the distance between CD and BC.

[2]Likewise in the following, unless explicitly stated otherwise, l_i ($i \in \{1, 2, 3\}$) is equivalent to $l_i(\theta, p)$ for the ease of presentation.

Then we have

$$F_{23}(d) = \frac{1}{S_2 S_3} \int_0^{\pi} \int_0^{p_m(\theta)} \left(F_{\mathcal{G}}^a(d) + F_{\mathcal{G}}^b(d) \right) \, \mathrm{d}p\mathrm{d}\theta, \quad (21)$$

where S_x is the area of $\mathcal{K}_x$. Meanwhile, with a weighted probabilistic sum, we have

$$F_{11}(d) = \frac{S_2}{S_1}(\underbrace{\frac{S_2}{S_1}F_{22}(d) + \frac{S_3}{S_1}F_{23}(d)}_{F_{12}(d)}) + \frac{S_3}{S_1}(\underbrace{\frac{S_2}{S_1}F_{23}(d) + \frac{S_3}{S_1}F_{33}(d)}_{F_{13}(d)}) . \quad (22)$$

With $F_{11}(d)$ and $F_{22}(d)$, and $F_{23}(d)$ obtained based on (13) and (21), respectively, $F_{12}(d)$, $F_{13}(d)$ (i.e., $F_V(d)$), and $F_{33}(d)$ (i.e., $F_U(d)$) can be obtained through (22). By considering the D2D communication range, $F_Q(d)$ can be obtained based on $F_U(d)$ using (15). Note that instead of using the probabilistic sum method, $F_{33}(d)$ can also be obtained by applying the approach introduced above for concave or disjoint geometries. With $F_{11}(d)$, $F_{22}(d)$, and $F_{33}(d)$ obtained, $F_{23}(d)$ can be obtained by using (22) instead of (21).

Note that if there are nodes uniformly deployed in $\mathcal{K}_2$ and $\mathcal{K}_3$ but with different node densities, the above weighted probabilistic sum is still applicable, but with the weights modified correspondingly due to the node density differences. Specifically, assuming the node density ratio between $\mathcal{K}_2$ and $\mathcal{K}_3$ is $\lambda_1 : \lambda_2$ (λ_1 and λ_2 are not zero at the same time),

$$F_{11}(d) = \sum_{i=2}^{3}\sum_{j=2}^{3} \frac{S_i \lambda_{i-1} S_j \lambda_{j-1}}{(\sum_{k=2}^{3} S_k \lambda_{k-1})^2} F_{ij}(d),$$

$$F_{1i}(d) = \sum_{j=2}^{3} \frac{S_j \lambda_{j-1}}{\sum_{k=2}^{3} S_k \lambda_{k-1}} F_{ij}(d), (i \in \{2,3\}). \quad (23)$$

Especially, if $\lambda_1 : \lambda_2 = 1 : 1$, i.e., both areas have the same node density, then $F_{11}(d)$ and $F_{1i}(d)$ ($i \in \{2,3\}$) are just what shown in (22). Therefore, our approach adopted in this paper has a potential of handling the networks with non-uniform nodal distributions.

C. Obtaining the SINR and Link Capacity Distributions

1) Signal or Interference Distribution: With the required distance distributions obtained above, the SINR distributions can be obtained according to (1)–(8). To this end, we first obtain the distribution of $d^{-\alpha}$ using the change-of-variable technique, based on which the distribution of the signal or interference from one source achieved at a receiver can be obtained. Specifically, let D be an RV of a distance with Probability Distribution Function (PDF) $f_D(d)$ defined over $d_1 \le d \le d_2$. A new RV, $D^{-\alpha}$, is introduced. Let $I = D^{-\alpha} = u(D)$, and $D = I^{-\frac{1}{\alpha}} = v(I)$. Then the CDF $F_I(i)$ defined over $u(d_2) \le i \le u(d_1)$ is

$$F_I(i) = \Pr(I \le i) = \Pr(u(D) \le i) = \Pr(D \ge v(i)) = 1 - \int_{d_1}^{v(i)} f_D(d) \, \mathrm{d}d. \quad (24)$$

Thus, the PDF is

$$f_I(i) = F_I'(i) = f_D(v(i)) \cdot |v'(i)| . \quad (25)$$

To obtain the distribution of cumulative interference from multiple sources, e.g., N DUE transmitters, the convolution operator is used for the PDF of the sum of independent RVs, as shown below in general,

$$I(x) = \psi^{(N)}(x), \quad (26)$$

where $I(x)$ represents the distribution of the total interference from all N DUE transmitters, and $\psi^{(z)}(\cdot)$ is the z-fold convolution of $\psi(\cdot)$.

2) SINR Distribution: In this subsection, we show in detail the analysis of the SINR distribution at the BS shown in (1) (the analysis is the same for the SINR distribution at a DUE receiver shown in (4)). Specifically, let the SINR at the BS obtained in (1) in dB be

$$S = 10\lg(SINR_B). \quad (27)$$

Obviously, S depends on the distance from the BS to the CUE (denoted as D, within the communication range $[d_{\min}, d_{\max}]$) and the cumulative interference from all DUE transmitters (denoted as I, $I \in [I_{\min}, I_{\max}]$). Let $f_D(d)$ and $f_I(i)$ denote the PDFs of D and I, respectively, which can be obtained following the approaches explained above.

Let $\mathtt{f}_S(D, I)$ represent the received SINR at the BS given that the distance between the CUE and the BS is D and the cumulative interference from all DUE transmitters to the BS is I, $\mathtt{f}_D(S, I)$ be the distance given the received SINR S and interference I, and $\mathtt{f}_I(S, D)$ be the interference given the received SINR S and distance D. Thus, $\mathtt{f}_S(d_{\max}, I_{\max}) \le S \le \mathtt{f}_S(d_{\min}, I_{\min})$. Then the CDF of the received SINR in dB at the BS is:

if $\mathtt{f}_S(d_{\max}, I_{\min}) \le \mathtt{f}_S(d_{\min}, I_{\max})$, then

$$\Pr(S \le s) = \begin{cases} \int_{\mathtt{f}_I(s,d_{\max})}^{I_{\max}} \int_{\mathtt{f}_D(s,i)}^{d_{\max}} f_D(d) f_I(i) \, \mathrm{d}d\mathrm{d}i, \\ \quad \text{if } \mathtt{f}_S(d_{\max}, I_{\max}) \le s \le \mathtt{f}_S(d_{\max}, I_{\min}), \\ \int_{I_{\min}}^{I_{\max}} \int_{\mathtt{f}_D(s,i)}^{d_{\max}} f_D(d) f_I(i) \, \mathrm{d}d\mathrm{d}i, \\ \quad \text{if } \mathtt{f}_S(d_{\max}, I_{\min}) \le s \le \mathtt{f}_S(d_{\min}, I_{\max}), \\ 1 - \int_{I_{\min}}^{\mathtt{f}_I(s,d_{\min})} \int_{d_{\min}}^{\mathtt{f}_D(s,i)} f_D(d) f_I(i) \, \mathrm{d}d\mathrm{d}i, \\ \quad \text{if } \mathtt{f}_S(d_{\min}, I_{\max}) \le s \le \mathtt{f}_S(d_{\min}, I_{\min}). \end{cases} , \quad (28)$$

otherwise,

$$\Pr(S \le s) = \begin{cases} \int_{\mathtt{f}_I(s,d_{\max})}^{I_{\max}} \int_{\mathtt{f}_D(s,i)}^{d_{\max}} f_D(d) f_I(i) \, \mathrm{d}d\mathrm{d}i, \\ \quad \text{if } \mathtt{f}_S(d_{\max}, I_{\max}) \le s \le \mathtt{f}_S(d_{\min}, I_{\max}), \\ \int_{d_{\min}}^{d_{\max}} \int_{\mathtt{f}_I(s,d)}^{I_{\max}} f_D(d) f_I(i) \, \mathrm{d}i\mathrm{d}d, \\ \quad \text{if } \mathtt{f}_S(d_{\min}, I_{\max}) \le s \le \mathtt{f}_S(d_{\max}, I_{\min}), \\ 1 - \int_{I_{\min}}^{\mathtt{f}_I(s,d_{\min})} \int_{d_{\min}}^{\mathtt{f}_D(s,i)} f_D(d) f_I(i) \, \mathrm{d}d\mathrm{d}i, \\ \quad \text{if } \mathtt{f}_S(d_{\max}, I_{\min}) \le s \le \mathtt{f}_S(d_{\min}, I_{\min}). \end{cases} . \quad (29)$$

Although the SINR distribution in closed form could not be obtained, with the developed numerical algorithm based on (28) and (29), we can obtain the corresponding numerical results promptly and accurately according to different network settings and parameters.

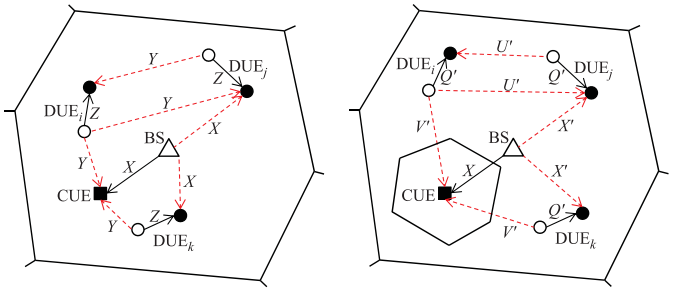

(a) No GR for the CUE (b) A GR for the CUE

Fig. 7. System model for the downlink reusing mode. The RVs, X, Y, and Z, are the same as those shown in Fig. 1.

3) Link Capacity Distribution: With the SINR distributions obtained above, the link capacity distributions can be obtained with (2) and (5) by using the change-of-variable technique. Specifically, let S be an RV of SINR with PDF $f_S(s)$ defined over $s_1 \le s \le s_2$. A new RV, $C = W \log_2(1+S)$, is introduced. Let $C = u(S)$, and $S = 2^{\frac{C}{W}} - 1 = v(C)$. Then the CDF $F_C(c)$ and PDF $f_C(c)$ defined over $u(s_1) \le c \le u(s_2)$ are respectively shown as

$$F_C(c) = \Pr(C \le c) = \Pr(u(S) \le c) = \Pr(S \le v(c)) = \int_{s_1}^{v(c)} f_S(s)\, \mathrm{d}s, \tag{30}$$

$$f_C(c) = F_C'(c) = f_S(v(c)) \cdot |v'(c)|. \tag{31}$$

V. Framework Applicability

A. Downlink Reusing Scenario

In an uplink reusing scenario, the D2D communications which are close to the BS may cause significant interference to the cellular communications due to the near-far effect [27]. Therefore, reusing downlink resources is also very important. The proposed framework can also be applied to a downlink reusing scenario, where concurrent D2D pairs will reuse the downlink resource of the BS, and thus the transmitting DUEs and BS can interfere with the reception at the CUE and the DUE receivers, respectively, as shown in Fig. 7. Accordingly, the received SINR at the CUE from the BS is

$$SINR_C = \frac{K P_B {d_0}^{\alpha} {d_{CUE,BS}}^{-\alpha}}{N_0 W + I_C}, \tag{32}$$

where P_B is the transmission power of BS, and I_C, the cumulative interference at the CUE, is

$$I_C = K P_D {d_0}^{\alpha} \sum_i {d_{DUE_{i\_TX},CUE}}^{-\alpha}. \tag{33}$$

Meanwhile, the received SINR at a DUE receiver in an arbitrary D2D pair, say pair i, can still be obtained according to (4), except that one of the two interference components in I_{Di}, i.e., I'_{Di} in (7) should be changed to

$$I'_{Di} = K P_B {d_0}^{\alpha} {d_{BS,DUE_{i\_RX}}}^{-\alpha}, \tag{34}$$

to represent the interference from the BS.

There are also two cases depending on whether a GR is set for the CUE to mitigate the interference from DUEs or not. For the case where there is no GR (e.g., Fig. 7(a)), all the involved distance distributions can be obtained using the approaches explained in Section IV-A and IV-B. As shown in Fig. 7, the RVs, X, Y, and Z, are the same as those shown in Fig. 1.

However, if there is a GR for the CUE and hence the D2D communications can only happen outside the GR (e.g., Fig. 7(b)), it becomes much more challenging to obtain the distributions of the distances involved in (4), (34), and (8), i.e., $d_{DUE_{i\_TX},DUE_{i\_RX}}$, $d_{BS,DUE_{i\_RX}}$ and $d_{DUE_{j\_TX},DUE_{i\_RX}}$, respectively, due to the randomness of the location of the GR for the CUE. Thus, it is difficult to obtain the distribution of the received SINR at a DUE receiver. But the distribution of the distance, $d_{CUE,BS}$, is still the same as that in the no-guard-region scenario, since the GR only affects the distribution of DUEs. Meanwhile, in a simple assumption where the GR is approximated by a circle with radius of R and centered at the CUE, the CDF of $d_{DUE_{i\_TX},CUE}$, $F_{V'}(d)$, can be obtained based on $F_Y(d)$ (which has been obtained in Section IV-B),

$$F_{V'}(d) = \frac{F_Y(d) - F_Y(R)}{1 - F_Y(R)}. \tag{35}$$

Therefore, the distribution of the received interference and SINR at the CUE can still be obtained.

B. Inter-Cell Interference in a Multi-Cell Network

If the frequency reuse factor in a cellular system is 1, i.e., all cells are using the same resources, it needs to take into consideration the interference from the UEs in neighbor cells. Then, we need to obtain the distributions of the distances from a BS in a cell to a UE in a different cell and from a DUE in a cell to a UE in a different cell. To obtain the former, our approach proposed in [16] still applies. For the latter, our approach proposed in [17] also applies, as illustrated in Fig. 5. As a result, the proposed framework in this paper can handle inter-cell interference in a multi-cell network.

C. Sector-Partitioned Cells

To increase the network capacity of a cellular system, equipping BSs with multiple directional antennas is a promising solution and has been actively studied and modeled for the throughput bound analysis on the underlaying D2D communications in [10]. With directional antennas, a cell can be divided into several smaller sections or so-called sectors, where it is possible for multiple CUEs to communicate with a BS simultaneously. Similarly, with our approaches proposed in [16] and [17] to the required distance distributions, the proposed framework can deal with sector-partitioned cells, whereby not only a single sector but also the inter-sector influence can be investigated, for both cellular and D2D communications, which would be a much further step compared to the D2D bound analysis in [10].

D. Irregular Cells and GRs

For the ease of presentation, in Section VI, the network performance is evaluated with a hexagonal cell and circular GR. However, as explained above, the proposed framework applies to the scenarios with irregular polygon-shaped cells and GRs. This is because both the underlying approaches to

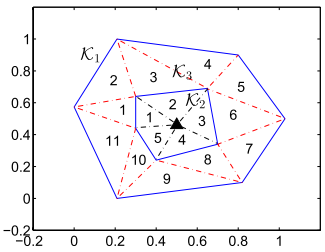

Fig. 8. An example of irregular cell $\mathcal{K}_1$ and GR $\mathcal{K}_2$, with the ring area labeled by $\mathcal{K}_3$ (▲: BS).

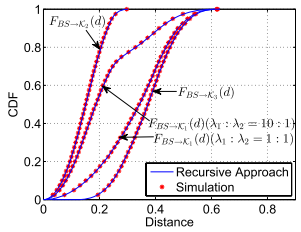

Fig. 9. Distributions of the distance from the BS to a random point associated with the irregular cell and GR shown in Fig. 8. $\lambda_1 : \lambda_2$ in (12) is set to $1 : 1$ or $10 : 1$.

obtaining the distributions of the distance between a given reference point and a random one (Ref2Ran), and that between two random points (Ran2Ran), can handle irregular polygons.

Figure 8 shows an example of irregular cell and GR for illustration. To obtain the required Ref2Ran distance distributions, as shown in Section IV-A, the triangulation with respect to the BS is adopted. For example, in Fig. 8, the area $\mathcal{K}_2$ is triangulated with respect to the BS with dashed black lines into 5 triangles. Then based on (9), the distribution of the distance from the BS to a random point in $\mathcal{K}_2$ is obtained (denoted as $F_{BS\to\mathcal{K}_2}(d)$, i.e., $F_G(d)$). In the same way, $F_{BS\to\mathcal{K}_1}(d)$ (i.e., $F_X(d)$) can be obtained. Then based on (12), $F_{BS\to\mathcal{K}_3}(d)$ (i.e., $F_W(d)$) can be obtained, assuming that the CUE appears in the areas of GR and $\widetilde{\text{GR}}$ with the same possibility (i.e., $\lambda_1 : \lambda_2 = 1 : 1$ in (12)). The obtained results are shown in Fig. 9.

To obtain the required Ran2Ran distance distributions, such as $F_{13}(d)$ (for obtaining $F_V(d)$) and $F_{33}(d)$ (for obtaining $F_U(d)$ and $F_Q(d)$), the ring area $\mathcal{K}_3$ is triangulated with dashed red lines into 11 triangles named by a number inside as shown in Fig. 8. As demonstrated in our technical report in [17], with the proposed approach we can obtain Ran2Ran distance distributions associated with arbitrary triangles, including the Ran2Ran distance distribution within an arbitrary triangle and that between two arbitrary triangles. Then with a probabilistic sum,

$$F_{33}(d) = \sum_{i=1}^{11}\sum_{j=1}^{11} \frac{S_i S_j}{(\sum_{k=1}^{11} S_k)^2} F_{ij}(d), \tag{36}$$

where S_x is the area of triangle x, and $F_{xy}(d)$ or $F_{yx}(d)$ is the CDF of the Ran2Ran distance distribution within triangle x if $x = y$, or between two triangles x and y if $x \neq y$. $F_{11}(d)$ and $F_{22}(d)$ can be obtained in the same way. Then based on (23), $F_{23}(d)$ and further $F_{13}(d)$ can be obtained, assuming that the CUE appears in the areas of GR and $\widetilde{\text{GR}}$ with the same possibility (i.e., $\lambda_1 : \lambda_2 = 1 : 1$ in (23)). The obtained results are shown in Fig. 10.

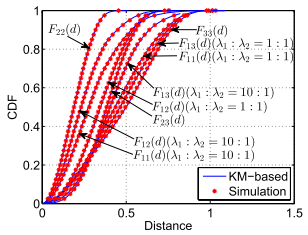

Fig. 10. Distributions of the distance between two random points associated with the irregular cell and GR shown in Fig. 8. $\lambda_1 : \lambda_2$ in (23) is set to $1 : 1$ or $10 : 1$.

E. Non-Uniform UE Distribution

If UEs are non-uniformly distributed in a cell, the cell area can be viewed in a different way, so that the non-uniform distribution can be considered as layers of uniform distributions, each of which can be addressed by the proposed framework. As an example, referring to the system model where a GR is set for the BS, DUEs are distributed in the cell but outside the GR. Therefore, the distribution of the DUEs is non-uniform in the entire cell, but is uniform in the cell minus the GR hole. On the other hand, it has a higher possibility that the UEs inside GR will choose the CUE mode than those inside $\widetilde{\text{GR}}$. Assuming such a probability ratio is $\lambda_1 : \lambda_2 = 10 : 1$, based on (12) and (23), we can obtain the corresponding distributions, which are different from those obtained when the probability ratio is $\lambda_1 : \lambda_2 = 1 : 1$, as shown in Fig. 9 and Fig. 10, respectively. Therefore, the proposed framework can also analyze the performance of the cellular network underlaying D2D communications with the non-uniform UE distribution described above.

VI. Performance Evaluation

In this section, the proposed framework is evaluated in terms of two important network metrics: cumulative interference and outage probability. The obtained numerical results from the framework are verified in comparison with simulations. Meanwhile, the effect of several system parameters on the performance metrics is investigated. The framework can provide insights when tuning the system parameters, e.g., the GR area for the BS and the number of concurrent D2D pairs, given the outage probability thresholds of both the BS and DUE receiver.

Considering the system model described in Section III, for the ease of presentation and WLOG, the cell is approximated as a regular hexagon with side length of 225 m and the GR for the BS as a circle with radius of R and centered at the BS. As explained earlier, the proposed approach does not impose any constraints on the shapes of the cell or GR. $W = 5$ MHz, $N_0 = -174$ dBm/Hz, $P_D = 2$ mWatt, $P_C = 0.2$ Watt, $d_{\min}^{D2D} = 2$ m, and $d_{\max}^{D2D} = 15$ m. The path-loss ratios are set as $L_{\text{B}}(d) = -128.1 - 20\lg(d/1000)$ (dB) for the BS-UE link, and $L_{\text{D}}(d) = -38 - 20\lg(d)$ (dB) for the DUE-DUE link [9]. So the path-loss exponent $\alpha = 2$. Numerical results are based on our analysis directly; on the other hand, the simulations are conducted in Matlab as follows:

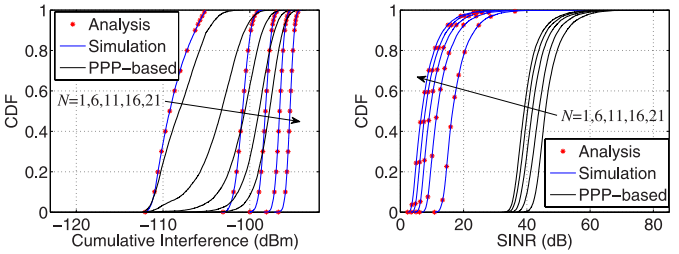

(a) Interference distribution (b) SINR distribution

Fig. 11. Distributions of the interference and SINR at the BS, with $R = 100$ m and $N = 1, 6, 11, 16,$ and 21.

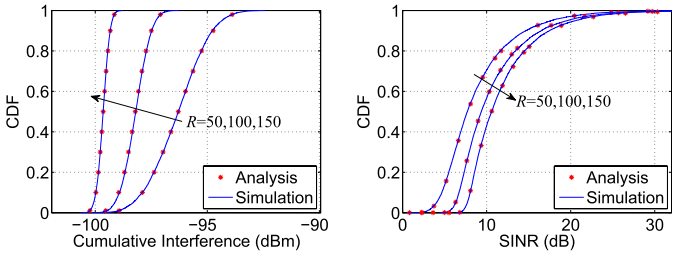

(a) Interference distribution (b) SINR distribution

Fig. 12. Distributions of the interference and SINR at the BS, with $N = 11$ and $R = 50, 100,$ and 150 m.

(1) Generate N concurrent D2D pairs and one CUE uniformly at random in the network.
(2) Compute the received interference and SINR at the CUE with the above network parameters and append the results to the interference matrix and SINR matrix, respectively.
(3) Compute the received interference and SINR at an arbitrary DUE receiver and append the computed results to another interference matrix and SINR matrix, respectively.
(4) Repeat steps (1)–(3) 50, 000 times (the more repeats, the more accurate the result). Then using the Matlab function "ecdf" with each matrix as its input, we can obtain the empirical CDFs of interference and SINR for both cellular and D2D communications.

Given a modulation and coding scheme, outage probability represents the chance that the SINR achieved at a receiver is no larger than a specified threshold and the reception is considered unsuccessful. Therefore, the CDF of the received SINR (as analyzed in Section IV-C) is significant to determine the outage probability of a system. Next, both the distributions of the cumulative interference and SINR at either the BS or a DUE receiver are shown, with the numerical results of our approach and the simulation results compared.

A. Distributions of Interference and SINR at the BS

We first evaluate the effect of the number of concurrent D2D pairs on the distributions of the interference and SINR received at the BS. With the GR radius R fixed to 100 m and the number of concurrent D2D pairs N varying from 1 to 21, the CDFs of the interference and SINR received at the BS are shown in Fig. 11(a) and Fig. 11(b), respectively. Obviously, given that the size of the GR is the same, more D2D pairs transmitting simultaneously can impose a higher interference on the BS, and thus the received SINR at the BS becomes lower, which increases its outage probability. As a result, for the interference distribution shown in Fig. 11(a), the CDF curves located on the right-hand side correspond to a larger N; while for the SINR distribution shown in Fig. 11(b), the CDF curves located on the left-hand side correspond to a larger N. Moreover, a good match between the simulation and analytical results can be observed in both figures. The results obtained based on the PPP model with the same node density are also shown for comparison. The implementation of the PPP model in Matlab is similar to the simulation implementation shown above, except that the number of nodes over all simulations follows a Poisson distribution. The comparison shows large gaps for both the interference and SINR achieved at the BS. Due to the border effect, PPP is inapplicable for the system model of finite networks used in this paper. In what follows, the comparison with PPP will be omitted.

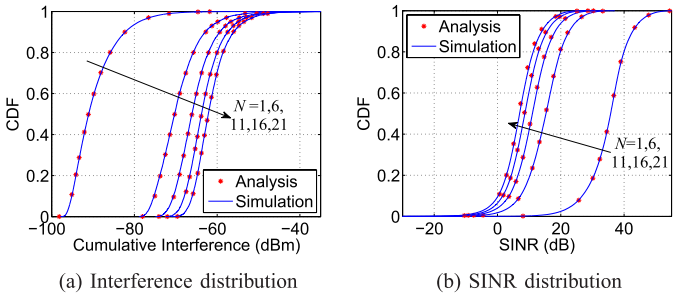

(a) Interference distribution (b) SINR distribution

Fig. 13. Distributions of the interference and SINR at a DUE receiver, with $R = 100$ m and $N = 1, 6, 11, 16,$ and 21.

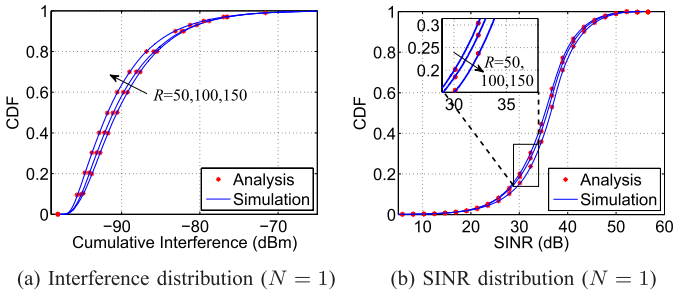

(a) Interference distribution ($N = 1$) (b) SINR distribution ($N = 1$)

Fig. 14. Distributions of the interference and SINR at a DUE receiver, with $N = 1$ and $R = 50, 100,$ and 150 m.

The effect of the GR size is also investigated. Specifically, with the number of concurrent D2D pairs fixed to $N = 11$ and the radius of the GR R varying from 50 to 150 m, Fig. 12(a) and Fig. 12(b) show the corresponding interference and SINR distributions, respectively. Intuitively, as the area of the GR for the BS increases, DUE transmitters are "pushed" farther away from the BS, and their cumulative interference to the reception at the BS decreases, and thus the received SINR at the BS becomes high, which decreases the outage probability of the BS, as shown in the figures.

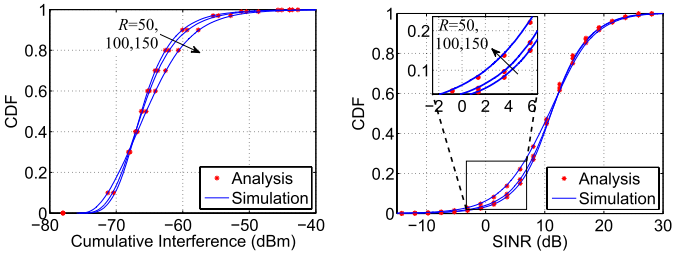

(a) Interference distribution ($N = 11$) (b) SINR distribution ($N = 11$)

Fig. 15. Distributions of the interference and SINR at a DUE receiver, with $N = 11$ and $R = 50$, 100, and 150 m.

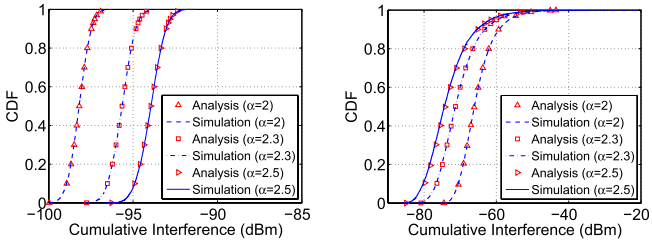

(a) Distribution of the interference at the BS (b) Distribution of the interference at a DUE receiver

Fig. 16. Interference distributions with $R = 100$ m, $N = 11$, and $\alpha = 2, 2.3$, and 2.5.

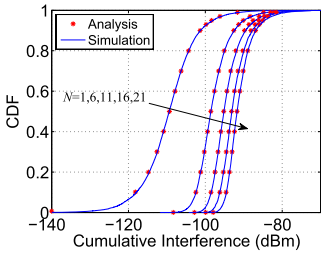

Fig. 17. Distributions of the interference at the BS from DUE transmitters with the Rayleigh fading effect considered ($R = 0$ m and $N = 1, 6, 11, 16$, and 21).

B. Distributions of Interference and SINR at a DUE Receiver

In this subsection, the distributions of the interference and SINR received at a DUE receiver in an arbitrary D2D pair are investigated. First, with $R = 100$ m and N varying from 1 to 21, the corresponding CDFs are shown in Fig. 13. When there is only one D2D pair, i.e., $N = 1$, the interference at the DUE receiver only comes from the CUE. As N increases, besides the interference from the CUE, a DUE receiver in a pair will also receive the interference from the DUE transmitters in all other D2D pairs, which leads to a shift of the CDF curves shown in Fig. 13(a) towards the arrow direction. Thus, the received SINR decreases, which increases the outage probability of the D2D communications, as shown in Fig. 13(b).

The effect of the GR size on the D2D communications is then investigated. We first fix $N = 1$, so only the CUE will interfere with the reception at the DUE receiver. As R increases from 50 to 150 m, the probability that there is a large distance between the CUE and the DUE receiver becomes higher, and thus the interference received at the DUE receiver decreases, as shown in Fig. 14(a), which correspondingly increases its received SINR and thus decreases the outage probability of the D2D communication, as shown in Fig. 14(b). In addition, from Fig. 14, we can observe that the GR size has a low impact on the D2D communication, as the DUE is less likely affected by a single CUE. Especially, when $R = 50$ and 100 m, the corresponding CDF curves of the SINR shown in Fig. 14(b) almost overlap with each other.

Then, we fix $N = 11$, so besides the interference from the CUE, an arbitrary D2D pair will also receive the interference from other 10 D2D pairs. The results are shown in Fig. 15. In contrast to the previous case where $N = 1$, as R increases, the cumulative interference to a D2D pair increases as well, as shown in Fig. 15(a), and thus the received SINR decreases, which increases the outage probability of D2D communications, as shown in Fig. 15(b). The results indicate that, with more concurrent D2D pairs, the interference to a D2D pair from all other D2D pairs will increase as the GR area increases, and such an increase dominates over the decrease of the interference from the CUE. Also, the CDFs for $R = 50$ and 100 m shown in Fig. 15 almost overlap with each other when DUEs are still sparsely spread out in the cell.

Figure 16 shows that distributions of the interference at the BS (Fig. 16(a)) and a DUE receiver (Fig. 16(b)), with $R = 100$ m, $N = 11$, and path-loss exponent $\alpha = 2, 2.3$, and 2.5. Since the BS-UE link and DUE-DUE link have different path-loss ratios due to antenna heights, the interference changes differently for the BS and a DUE receiver as α increases.

All the results shown above in a close match with the simulation results demonstrate the accuracy of our approach. Based on our performance studies, the proposed analytical framework in this paper can be used to guide the planning and dimensioning at the system level, e.g., on average, how large N is allowed to be and how R is set by considering the bounded outage probabilities for both cellular and D2D communications systematically and comprehensively.

It is worth noting that the proposed model can be readily extended to include the shadowing and fading effects of wireless channels. For example, log-normal shadowing and Rayleigh fading can be considered [29]. For the Rayleigh fading channel given the distance between a transmitter and receiver as d, we have the PDF of the channel power gain as

$$f_X(x|d) = \frac{1}{P_t K (d_0/d)^{\alpha}} \mathrm{e}^{\frac{-x}{P_t K (d_0/d)^{\alpha}}}, \tag{37}$$

where P_t is the transmission power of transmitter, K is the antenna- and processing gain-related parameter, d_0 is the reference distance. Then the PDF of the signal achieved at the receiver is

$$f_X(x) = \int_{d_{\min}}^{d_{\max}} f_X(x|d) f_D(d) \mathrm{d}d, \tag{38}$$

where $f_D(d)$ is the PDF of any distance distribution shown in Table I, and $d_{\min}$ and $d_{\max}$ are the minimum and maximum distances between the transmitter and receiver, respectively. Take the interference from DUE transmitters to the BS in the uplink resource reusing scenario for example, with the Rayleigh fading effect considered, Fig. 17 shows the CDFs

of the interference received at the BS. In addition, log-normal shadowing and Rayleigh fading can also be modeled as independent random variables that are not related to inter-node distances. As shown in [28], the shadowing effect follows a log-normal distribution with standard deviation σ (typically between 0 and 8 dB), and Rayleigh fading follows an exponential distribution of mean 1. Therefore, the extension of the path-loss model along with shadowing and fading is the multiplication of independent random variables and can still be analyzed based on the proposed framework.

VII. Conclusions

This paper presented an analytical framework based on a probabilistic distance and path-loss model for the performance analysis in a cellular network with underlaying D2D communications. To this end, we first obtained the distance distributions associated with arbitrarily-shaped polygons with and without a hole inside, including the distributions of the distance from a given reference point to a random one and that between two random points. Utilizing these distance distributions in a general path-loss model, we then derived the distributions of the received signal, interference, and further SINR. Based on the obtained results, the interference and outage probabilities for both the cellular and D2D communications in an uplink reusing scenario are thoroughly investigated. The accurate analysis demonstrated the promising potentials of the proposed framework, which we believe is a significant complementary work to the existing approaches and results, and can provide meaningful insights and guidelines for the design and optimization of D2D communications in the next-generation cellular networks. Based on the proposed framework, further investigation can be done for modeling and analyzing the downlink reusing scenario, the multi-cell scenarios, and the non-uniform distribution of UEs, considering other channel impairments such as shadowing and fast fading.

References

[1] Cisco Visual Networking Index, "Global mobile data traffic forecast update, 2015–2020," Cisco Vis. Netw. Index, White Paper, Feb. 2015. [Online]. Available: https://goo.gl/zUrZ5q

[2] P. Bahl, R. Chandra, T. Moscibroda, R. Murty, and M. Welsh, "White space networking with Wi-Fi like connectivity," in *Proc. ACM SIGCOMM*, 2009, pp. 27–38.

[3] C.-H. Lee and M. Haenggi, "Interference and outage in Poisson cognitive networks," *IEEE Trans. Wireless Commun.*, vol. 11, no. 4, pp. 1392–1401, Apr. 2012.

[4] J. G. Andrews, H. Claussen, M. Dohler, S. Rangan, and M. C. Reed, "Femtocells: Past, present, and future," *IEEE J. Sel. Areas Commun.*, vol. 30, no. 3, pp. 497–508, Apr. 2012.

[5] A. Asadi, Q. Wang, and V. Mancuso, "A survey on device-to-device communication in cellular networks," *IEEE Commun. Surveys Tut.*, vol. 16, no. 4, pp. 1801–1819, 4th Quart., 2014.

[6] Y. Cheng, H. Han, and X. Lin, "Device-to-device communication in CDMA-based cellular systems—Uplink capacity analysis," in *Proc. IEEE Commun. Softw. Netw.*, May 2011, pp. 430–434.

[7] H. Min, J. Lee, S. Park, and D. Hong, "Capacity enhancement using an interference limited area for device-to-device uplink underlaying cellular networks," *IEEE Trans. Wireless Commun.*, vol. 10, no. 12, pp. 3995–4000, Dec. 2011.

[8] R. Chen, X. Liao, S. Zhu, and Z. Liang, "Capacity analysis of device-to-device resource reusing modes for cellular networks," in *Proc. IEEE ComNetSat*, Jul. 2012, pp. 64–68.

[9] M. Ni, L. Zheng, F. Tong, J. Pan, and L. Cai, "A geometrical-based throughput bound analysis for device-to-device communications in cellular networks," *IEEE J. Sel. Areas Commun.*, vol. 33, no. 1, pp. 100–110, Jan. 2015.

[10] M. Ni, J. Pan, and L. Cai, "Geometrical-based throughput analysis of device-to-device communications in a sector-partitioned cell," *IEEE Trans. Wireless Commun.*, vol. 14, no. 4, pp. 2232–2244, Apr. 2015.

[11] C. Ma, W. Wu, Y. Cui, and X. Wang, "On the performance of successive interference cancellation in D2D-enabled cellular networks," in *Proc. IEEE INFOCOM*, Apr./May 2015, pp. 37–45.

[12] X. Xu, H. Wang, H. Feng, and C. Xing, "Analysis of device-to-device communications with exclusion regions underlaying 5G networks," *Trans. Emerg. Telecommun. Technol.*, vol. 26, no. 1, pp. 93–101, Jan. 2015.

[13] J. Li, W. Xia, and L. Shen, "Delay-aware resource control for device-to-device underlay communication systems," *Trans. Emerg. Telecommun. Technol.*, to be published. [Online]. Available: https://goo.gl/tQqXvS

[14] J. Wang, D. Zhu, C. Zhao, J. C. F. Li, and M. Lei, "Resource sharing of underlaying device-to-device and uplink cellular communications," *IEEE Commun. Lett.*, vol. 17, no. 6, pp. 1148–1151, Jun. 2013.

[15] D. Feng, L. Lu, Y. Yuan-Wu, G. Y. Li, G. Feng, and S. Li, "Device-to-device communications underlaying cellular networks," *IEEE Trans. Commun.*, vol. 61, no. 8, pp. 3541–3551, Aug. 2013.

[16] M. Ahmadi and J. Pan, "Random distances associated with arbitrary triangles: A recursive approach with an arbitrary reference point," in *Proc. UVicSpace*, 2014. pp. 1–13. [Online]. Available: http://hdl.handle.net/1828/5134

[17] F. Tong and J. Pan, "Random distances associated with arbitrary polygons: An algorithmic approach between two random points," Jan. 2016. [Online]. Available: https://arxiv.org/abs/1602.03407

[18] H. de H. M. Barros, M. G. S. Rêgo, E. O. Lucena, T. F. Maciel, W. C. Freitas, Jr., and F. R. P. Cavalcanti, "A distance-based study for device-to-device communication underlaying a cellular system," in *Proc. Simpósio Brasileiro Telecomun. (SBRT)*, 2012, pp. 1–5.

[19] Z.-S. Syu and C.-H. Lee, "Spatial constraints of device-to-device communications," in *Proc. BlackSeaCom*, Jul. 2013, pp. 94–98.

[20] M. Ahmadi, M. Ni, and J. Pan, "A geometrical probability-based approach towards the analysis of uplink inter-cell interference," in *Proc. IEEE GLOBECOM*, Dec. 2013, pp. 4952–4957.

[21] J. Guo, S. Durrani, and X. Zhou, "Outage probability in arbitrarily-shaped finite wireless networks," *IEEE Trans. Commun.*, vol. 62, no. 2, pp. 699–712, Feb. 2014.

[22] M. Ahmadi, F. Tong, L. Zheng, and J. Pan, "Performance analysis for two-tier cellular systems based on probabilistic distance models," in *Proc. IEEE INFOCOM*, Apr./May 2015, pp. 352–360.

[23] A. Goldsmith, *Wireless Communications*. Cambridge, U.K.: Cambridge Univ. Press, 2005.

[24] L. A. Santaló, *Integral Geometry and Geometric Probability*. Cambridge, U.K.: Cambridge Univ. Press, 2004.

[25] F. Piefke, "Beziehungen zwischen der sehnenlängenverteilung und der verteilung des abstandes zweier zufälliger punkte im eikörper," *Probab. Theory Rel. Fields*, vol. 43, no. 2, pp. 129–134, 1978.

[26] T. Koshizuka and S. Ohtsu, "Distance distribution in an arbitrary region and its application to the daily trip in Tokyo," *Urban Planning Soc. Jpn.*, vol. 36, pp. 871–876, 2001. [Online]. Available: http://hdl.handle.net/10252/4955

[27] D. Zhu, J. Wang, A. L. Swindlehurst, and C. Zhao, "Downlink resource reuse for device-to-device communications underlaying cellular networks," *IEEE Signal Process. Lett.*, vol. 21, no. 5, pp. 531–534, May 2014.

[28] D. Ben Cheikh, J.-M. Kelif, M. Coupechoux, and P. Godlewski, "SIR distribution analysis in cellular networks considering the joint impact of path-loss, shadowing and fast fading," *EURASIP J. Wireless Commun. Netw.*, vol. 2011, no. 1, pp. 1–10, Dec. 2011. [Online]. Available: https://goo.gl/5AUEdC

[29] L. Zheng, N. Lu, and L. Cai, "Reliable wireless communication networks for demand response control," *IEEE Trans. Smart Grid*, vol. 4, no. 1, pp. 133–140, 2013.

Fei Tong (S'13) received the bachelor's degree in computer science and technology from South-Central University for Nationalities, Wuhan, China, in 2009, and the M.E. degree in computer engineering from Chonbuk National University, Jeonju, South Korea, in 2011. He is currently pursuing the Ph.D. degree with the Department of Computer Science, University of Victoria, Victoria, Canada. His current research interests include protocol design and performance analysis for advanced wireless networking.

Ying Wan received the bachelor's degree in communications engineering from Northwestern Polytechnical University, Xi'an, China, in 2016. He is currently pursuing the Ph.D. degree with the Department of Computer Science, Tsinghua University, Beijing, China. His current research interests include named data networking and vehicular networks.

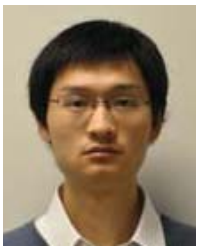

Lei Zheng received the B.S. and M.S. degrees in electrical engineering from the Beijing University of Posts and Telecommunications, Beijing, China, in 2007 and 2010, respectively, and the Ph.D. degree in electrical and computer engineering from the University of Victoria in 2014. His research interest is machine-to-machine networks, including medium access control protocol, radio resource allocation in wireless networks, and demand response control in Smart Grid.

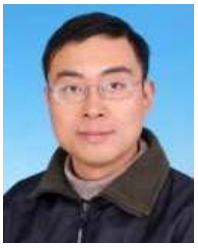

Jianping Pan (S'96–M'98–SM'08) is currently a Professor of Computer Science with the University of Victoria, Victoria, BC, Canada. He received the bachelor's and Ph.D. degrees in computer science from Southeast University, Nanjing, Jiangsu, China. He was a Post-Doctoral Researcher with the University of Waterloo, Waterloo, ON, Canada. He was with the Fujitsu Laboratories and NTT Laboratories. His area of specialization is computer networks and distributed systems, and his current research interests include protocols for advanced networking, performance analysis of networked systems, and applied network security. He received the IEICE Best Paper Award in 2009, the Telecommunications Advancement Foundations Telesys Award in 2010, the WCSP 2011 Best Paper Award, the IEEE GLOBECOM 2011 Best Paper Award, the JSPS Invitation Fellowship in 2012, and the IEEE ICC 2013 Best Paper Award. He is serving on the technical program committees of major computer communications and networking conferences including the IEEE INFOCOM, the ICC, the GLOBECOM, the WCNC, and the CCNC. He is the Ad Hoc and Sensor Networking Symposium Co-Chair of the IEEE GLOBECOM 2012 and an Associate Editor of the IEEE TRANSACTIONS ON VEHICULAR TECHNOLOGY. He is a senior member of the ACM.

Lin Cai (S'00–M'06–SM'10) received the M.A.Sc. and Ph.D. degrees in electrical and computer engineering from the University of Waterloo, Waterloo, ON, Canada, in 2002 and 2005, respectively. Since 2005, she has been an Assistant Professor and a Professor with the Department of Electrical and Computer Engineering, University of Victoria, Victoria, BC, Canada. Her research interests include wireless communications and networking, with a focus on network protocol design and control strategy supporting emerging applications in ubiquitous networks. She has been an Associate Editor of the IEEE TRANSACTIONS ON WIRELESS COMMUNICATIONS, the IEEE TRANSACTIONS ON VEHICULAR TECHNOLOGY, *EURASIP Journal on Wireless Communications and Networking*, the *International Journal of Sensor Networks*, and the *Journal of Communications and Networks*.